

Interplay of local and global interfacial electronic structure of a strongly coupled dipolar organic semiconductor

Nahid Ilyas and Oliver L. A. Monti*

Department of Chemistry & Biochemistry, University of Arizona, 1306 E. University Blvd., Tucson, Arizona 85721, USA

(Received 25 July 2014; published 22 September 2014)

We investigate the consequences of strong electronic coupling at the organic semiconductor/metal interface in both the ground and excited state manifold for the case of chloro-boron subphthalocyanine on Cu(111). Using a combination of low-temperature scanning tunneling microscopy and ultraviolet photoelectron spectroscopy and angle-resolved two-photon photoemission, we are able to connect local electronic interactions at the interface with thin film structure despite complex growth in the submonolayer regime. We show that strong coupling leads to charge transfer from the surface to the molecule, and we are able to correlate this observation with the specific molecular adsorption geometry. Strong coupling further results in molecular excited state anion resonances and is responsible for autoionization of highly excited image potential states, relating to the heterogeneous electronic environment in these thin films. This study provides a step towards disentangling interfacial electronic interactions at complex organic/metal interfaces.

DOI: [10.1103/PhysRevB.90.125435](https://doi.org/10.1103/PhysRevB.90.125435)

PACS number(s): 71.20.Rv, 79.60.Fr, 79.60.Jv, 68.37.Ef

I. INTRODUCTION

Interfaces of organic semiconductors with metals exhibit rich physics due to the interplay of the localized molecular electronic structure and the delocalized band structure of the supporting surface [1]. Both short-range and long-range interactions can play an important role, making it at present still difficult to predict or rationally design a desired energy-level alignment at such an interface [2,3]. Further complications arise from an often rich and complex landscape of organic film growth and self-assembly at the metal surface [4], since the interfacial properties arise due to both surface/molecule and molecule/molecule interactions [5,6]. This is further accentuated in the case of strong coupling, where charge transfer across the interface can have a substantial impact on the interfacial energy-level alignment [7–10].

Notably missing is a close connection between the electronic structure and self-assembly at the surface. The structure is often inferred spectroscopically [11–13], an approach that works well for highly ordered organic thin films such as, e.g., C₆₀ on Cu(111) [14] or perylene-3,4,9,10-tetracarboxylic dianhydride (PTCDA) on Ag(111) [9]. More commonly though, organic thin film growth can be rather complex [15], and mechanisms of establishing the interfacial electronic structure must be inferred somewhat indirectly. Importantly, in such films the electronic structure can be expected to vary locally, and as a result, disentangling the energetics in photoelectron spectroscopy is usually challenging. The combination of photoelectron spectroscopy with scanning tunneling microscopy (STM) provides, however, a powerful approach towards connecting film and electronic structure. Such characterization of the varying local electronic environment, particularly at a strongly coupled organic/metal interface, is thus a key step in understanding the energy-level alignment and carrier dynamics in systems with complex film structure. For example, in organic electronic devices

where films are frequently prepared under less controlled conditions, inhomogeneous film growth can be expected to lead to different energy-level alignment in microscopically different regions of the interface, giving rise to active vs inactive sites and likely different carrier dynamics [16]. Hence, systematic studies connecting thin film growth at a molecular level and electronic structure in films of model organic semiconductors on metal surfaces are needed in order to reveal the relevant driving forces for establishing interfacial energy-level alignment.

Here, we investigate the electronic interactions of a dipolar organic semiconductor, chloro-boron subphthalocyanine (ClB-SubPc) with Cu(111). The combination of low-temperature scanning tunneling microscopy (LT-STM), valence band photoemission analysis from ultraviolet photoelectron spectroscopy (UPS), and two-photon photoemission (TPPE) enables us to obtain detailed information of the interface, electronic structure, and its dependence on thin film structure despite complex polymorphic thin film growth. We are able to unravel the rich spectroscopy of this organic/metal interface to reveal the presence and origin of strong electronic coupling between surface and molecule. We show that a subset of ClB-SubPc molecules undergoes a significant charge transfer upon adsorption on Cu(111). This interaction is detected from (i) a newly occupied state arising near the Fermi level and (ii) autoionization of an image potential state (IPS) of Cu(111) into the continuum above ClB-SubPc islands.

This paper is organized as follows: In Sec. II, we provide the details of the experimental procedures for UPS, TPPE, and STM measurements. The molecular growth determined from STM images is presented in Sec. III, and it is related to the interfacial electronic structure observed at various surface coverages. Section IV contains a detailed analysis and discussion of the surface/molecule coupling, the complex interfacial electronic structure arising from the polymorphous thin film growth, and the influence of the varying local vacuum level on the surface/molecule interactions. A brief summary of important findings from the TPPE, UPS, and STM results concludes the report.

*monti@u.arizona.edu

II. EXPERIMENTAL

The polished Cu(111) crystal was purchased from Princeton Scientific (99.999% purity) and cleaned by repeated cycles of argon ion sputtering and annealing. CIB-SubPc was purchased from Sigma-Aldrich and was purified by gradient sublimation in a custom-built furnace, followed by degassing in a home-built Knudsen cell overnight under ultrahigh vacuum (UHV) conditions and at temperatures slightly below sublimation.

Analysis of the electronic structure of the CIB-SubPc films was performed with a photoelectron spectrometer (VG EscaLab MK II) equipped with an integrated sample heater and operated under UHV conditions at a base pressure of 2×10^{-10} Torr. All spectra were acquired at room temperature. CIB-SubPc films were analyzed using He(I) UPS (SPECS UVS 10/35, 30° angle of incidence from normal) to determine the global vacuum level at the interface and to determine occupied levels such as the highest occupied molecular orbital (HOMO), etc. The interfacial electronic structure of CIB-SubPc/Cu(111) was investigated by angle-resolved TPPE (AR-TPPE) with a tunable femtosecond laser system, which consists of a Ti:sapphire oscillator (80 MHz repetition rate, 100 fs pulse duration) frequency-doubled and frequency-tripled to obtain photon energies in the range of 2.61–5.10 eV. The ultrafast laser pulses were compressed in prism pairs and introduced into the UHV chamber through a fused silica viewport. In order to avoid space-charging and photoinduced sample damage, the pulse energy was kept at or below 350 pJ. The energy and angular resolution of the photoelectron spectrometer were 89(8) meV and 1.5° , respectively. During deposition of organic molecules, the substrate was kept at room temperature, and the CIB-SubPc surface coverage was determined by a custom-built quartz crystal microbalance calibrated separately in the STM chamber. All photoemission feature energies are reported as peak centers.

STM measurements were carried out in a separate UHV system (base pressure $< 1 \times 10^{-10}$ Torr) equipped with a low-temperature STM (modified CreaTech with GXSM custom control [17]). Purified CIB-SubPc molecules were sublimated onto Cu(111) held at 205 K or room temperature in a separate preparation chamber, and the sample was subsequently transferred to the cooled microscope head. All STM images were obtained using electrochemically etched tungsten tips in constant-current mode at 5 K. Coverage-dependent and temperature-dependent STM experiments showed no evidence of dissociation of the Cl atom from CIB-SubPc on Cu(111). The molecular film thickness was determined from statistical analysis of STM images at low coverages. A monolayer of CIB-SubPc refers to a putative idealized full monolayer, self-assembled in the high-density hexagonally close-packed structure (see below). All CIB-SubPc/Cu(111) coverages in both STM and TPPE analysis are reported in terms of monolayer equivalent (MLE) based on this analysis.

As shown in Fig. 1, TPPE probes both occupied and unoccupied states. Occupied electronic states below the Fermi level, $|i\rangle$, are ionized by coherent absorption of two photons. Unoccupied excited states, $|interm.\rangle$, are initially populated by photoexcitation, followed by absorption of a second photon and photoemission. In case the photon energy equals the energy difference between an occupied state and an unoccupied state, an optical resonance (direct resonance)

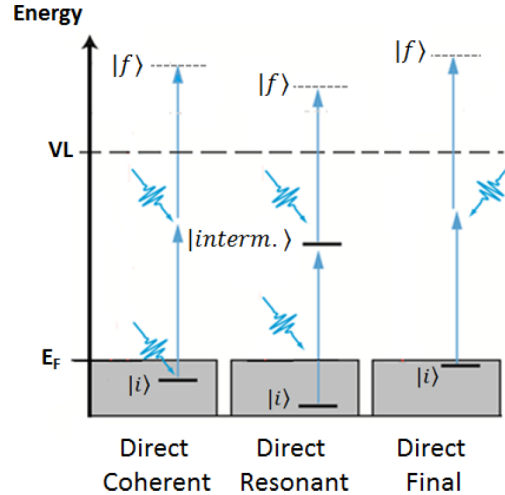


FIG. 1. (Color online) Schematic of single-color two-photon processes in TPPE experiments. Occupied states $|i\rangle$ below the Fermi level are photoionized by coherent absorption of two photons, while photoemission from excited states $|interm.\rangle$ requires a single photon only. Final state resonances are located above the local vacuum level and autoionize without further light absorption.

may occur, which manifests itself by a resonance-sharpened spectral line shape [18,19]. Finally, discrete final states, $|f\rangle$, are located above the local vacuum level and are probed by direct absorption of two photons, subsequently decaying by autoionization.

Unlike UPS, the kinetic energies measured by TPPE are not directly converted into binding energies, since both occupied and unoccupied states appear experimentally on the same kinetic energy axis. In order to decompose the TPPE spectra, the kinetic energies are converted to final state energies, i.e., reported as energy above the Fermi level after photon absorption and photoemission. Subsequently, the nature of each spectral feature is assigned by the following procedure: When excitation energies are varied in TPPE, electronic states exhibit different behavior depending on their electronic origin. States below the Fermi level are photoionized by absorption of two photons simultaneously, which is reflected in TPPE spectra as “two-photon dependence” of the final state energy shift Δ with excitation energy: $\Delta = 2 \times |h\omega_i - h\omega_j|$, where $h\omega_i$ and $h\omega_j$ refer to any two different excitation energies available from the tunable light source in TPPE. In contrast, only the absorption of the second photon results in the photoionization of unoccupied states, and the final state energy shifts only by $\Delta = |h\omega_i - h\omega_j|$ (“one-photon dependence”) with a change in excitation energy. Discrete states above the vacuum level (final state resonances) display no photon energy dependence ($\Delta = 0$) in TPPE spectra, as they are already above the vacuum level and in resonance with the continuum. Note that such simple photon-energy dependencies are not appropriate for transitions involving bulk states due to the conservation of all electron momentum components [20].

The dispersion of states was measured in AR-TPPE by restricting the analyzer acceptance angle to 1.5° . The sample was rotated along an axis perpendicular to the principal spectrometer axis. Since the parallel component of the

electron momentum, k_{\parallel} , is conserved during the photoemission process, the kinetic energy E_{kin} of photoelectrons is related to k_{\parallel} by

$$k_{\parallel} = \frac{\sqrt{2m_e E_{\text{kin}}}}{\hbar} \sin \theta, \quad (1)$$

where m_e represents the electron mass in vacuum, and θ indicates the emission angle relative to the surface normal.

III. RESULTS

We first briefly discuss the growth of the adsorbate on the surface in order to understand the molecular organization, since we will show below that this directly impacts the interfacial electronic structure. We then proceed to present the spectroscopic results from TPPE measurements, so as to disentangle the complex surface/molecule interactions in order to connect thin film structure and photoemission spectroscopy results.

A. Film growth and structure

In order to investigate the film growth and adsorption geometry of ClB-SubPc on Cu(111), we performed a series of STM experiments on submonolayer films prepared under a wide range of conditions. Identification of the preferred adsorption geometries of the molecules on the surface was accomplished by first examining conditions with minimal direct intermolecular interactions. Figure 2 shows a sample STM image of 0.04 MLE ClB-SubPc on Cu(111), prepared at 205 K. The triangular-shaped molecules appear as bright protrusions and exhibit two different contrasts in constant-current STM images. These can be associated with two types of adsorption geometries: Molecules with high electron density in the center are assigned as “Cl-up” (Cl facing vacuum), while the configuration with lower density in the molecular center corresponds to “Cl-down” (Cl facing surface). In both orientations, the C_3 molecular axis is oriented perpendicular to the surface. These two geometries are generally the only ones found on the surface, and they are sufficient to describe the self-assembly and film structure at higher coverage and room temperature as well.

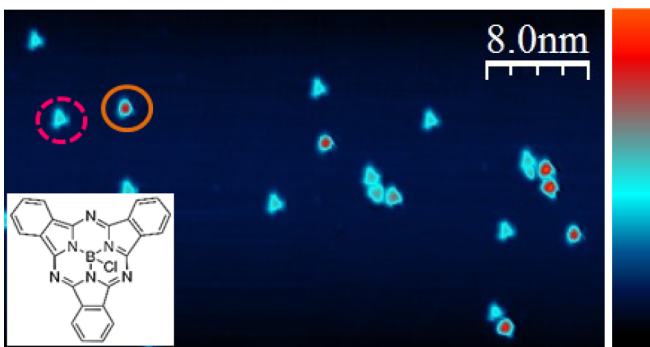


FIG. 2. (Color online) Constant-current STM image of 0.04 MLE ClB-SubPc measured at 5 K (sample bias $V_s = -2.0$ V, current $I = 50$ pA, surface prepared at 205 K) showing different imaging contrast for Cl-up (orange solid circle) and Cl-down (pink dashed circle) orientations. The inset shows the molecular structure.

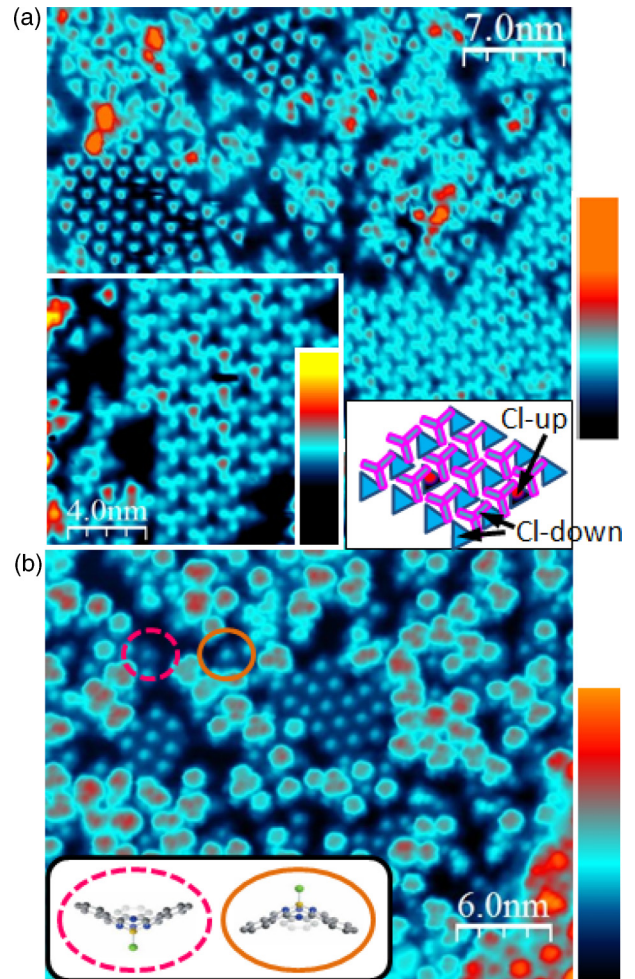


FIG. 3. (Color online) Constant-current STM images of ClB-SubPc on Cu(111) measured at 5 K. (a) 0.50 MLE surface coverage ($V_s = -2$ V, $I = 50$ pA, film prepared at 205 K) showing hexagonal packing of Cl-up molecules and bilayer structure formed by stacking of Cl-down molecules (insets). In the bilayer islands, the molecular contrast of the Cl-down molecules in the second layer (purple trileaf) significantly differs from those Cl-down molecules in the first monolayer (blue triangle) and in isolation. (b) 0.76 MLE surface coverage ($V_s = -2$ V, current $I = 50$ pA, film prepared at room temperature).

Figure 3 shows constant-current STM images of ClB-SubPc on Cu(111) at higher surface coverages. In both films [Fig. 3(a), 0.47 MLE, prepared at 205 K; Fig. 3(b), 0.76 MLE, prepared at room temperature], inhomogeneous film growth is observed. Ordered islands coexist along with disordered two-dimensional (2D) and three-dimensional (3D) structures. The molecular organization shows strong orientation dependence in the formation of the ordered islands. For growth at 205 K, both molecular orientations (Cl-up and Cl-down) participate in island formation; however, while Cl-up molecules tend to form hexagonal 2D islands, Cl-down molecules stack together in a staggered bilayer structure mixed with some Cl-up molecules interspersed [see Fig. 3(a) inset and diagram]. For this coverage and preparation temperature, taller or disordered clusters are rare. In contrast, films prepared at room temperature do not grow layer by layer; rather, orientation-selective adsorption

of CIB-SubPc on Cu(111) is observed [Fig. 3(b)], where the Cl-up orientation dominates in the first layer, as evidenced from the molecular contrast in STM images and the formation of 2D hexagonal islands. No evidence for Cl-down bilayers is observed, and Cl-down species in this and all other images taken of films prepared under these conditions are rare and occur mostly in isolation. Larger clusters with somewhat ill-defined molecular geometries grow on top of the Cl-up wetting layer, still visible beneath and at the edges of these clusters.

The LT-STM data show therefore that room-temperature-grown films are dominated by a Cl-up wetting layer. In addition, both patches of bare Cu(111) and multilayer clusters without clearly defined molecular adsorption structure are also present. At lower temperature and coverage, films grow in a more ordered fashion with multiple different preferred island structures. This understanding forms the basis for investigations of the interfacial electronic structure in the remainder of the study.

B. Electronic structure

With an understanding of the complex and heterogeneous growth for several different coverages in hand, we turn our attention to the interfacial electronic structure. In this section, we first present an overview and assignment of the observed features in the photoemission spectra, including the work function evolution. This overview will already indicate the presence of strong interface coupling, which will then be discussed in more detail in Sec. IV.

1. Evolution of the work function

The work function, measured at the secondary electron cutoff in photoelectron spectroscopy as a *global* work function [21], exhibits the balance between various forces that increase or decrease the vacuum level of a system upon molecular adsorption [5,22,23]. Molecular dipole moment [11,24], electron transfer from surface to molecule and chemisorption, [25,26] as well as pushback effects [27] can all contribute to the work function change upon film growth. The work function evolution gives thus a first clue to the surface/molecule interactions.

Figure 4 shows the coverage-dependent evolution of the global work function as measured by UPS of CIB-SubPc on Cu(111). The interface clearly develops a strong interface dipole, saturating only near 2 MLE (see Fig. 4). This is indicative of an at least partially heterogeneous 3D growth mode and in agreement with LT-STM for room-temperature-grown films [Fig. 3(b)].

An overview of the evolution of the interfacial electronic structure, measured by TPPE at an excitation energy of 3.31 eV and ranging from submonolayer to multilayer coverage, is shown in Fig. 5. The assignments discussed next arise from consistent global fits of the AR-TPPE spectra acquired in the range of 3.1–3.4 eV and 4.0–4.5 eV and the two different coverages also studied by LT-STM. There are altogether six distinctive features that show up at this and all other excitation energies investigated, discussed in the following sections.

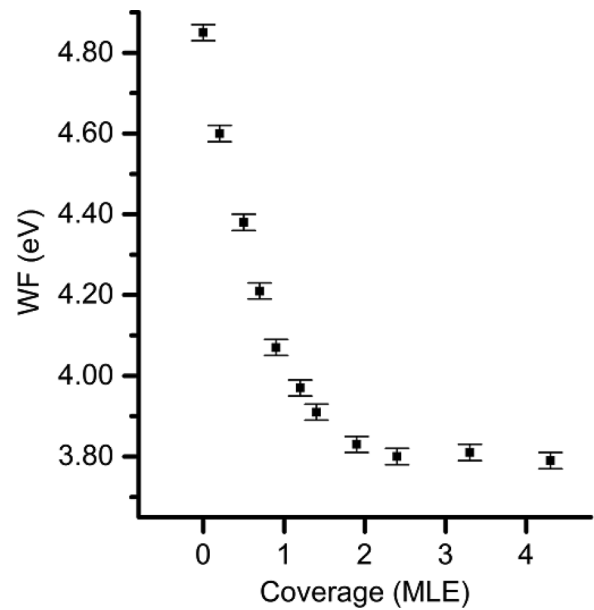


FIG. 4. Work function evolution tracked by UPS measurements taken at various CIB-SubPc coverages on Cu(111).

2. Shockley surface state

The Shockley surface state is strongly visible on bare Cu(111) at a final state energy of 6.31(2) eV [binding energy of $-0.31(2)$ eV], and it broadens somewhat at low coverage (0.47 MLE) while remaining dispersive [Fig. 6(a)] in the surface plane with an effective mass of $m_{\text{eff}} \approx 0.4m_e$. This assignment is also consistent with both a two-photon

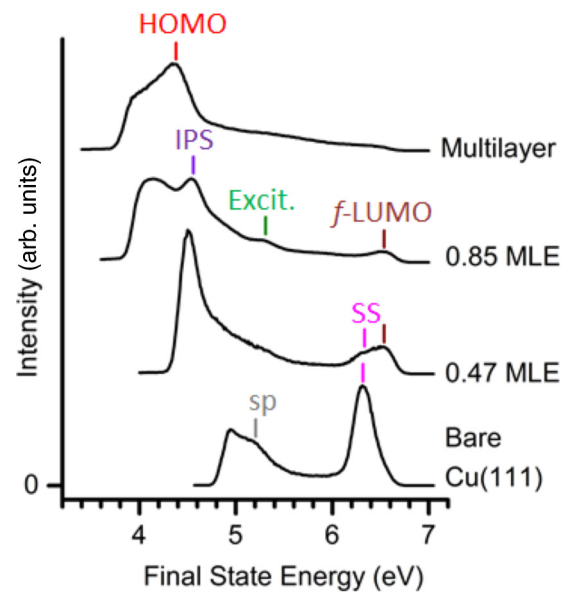


FIG. 5. (Color online) TPPE spectra of CIB-SubPc/Cu(111) measured with $\hbar\omega = 3.31$ eV showing the presence of both surface and molecular electronic states at various surface coverages. sp: Cu bulk *sp* band. SS: Shockley surface state. *f*-LUMO: filled lowest unoccupied molecular orbital. Excit.: excited states. IPS: image potential state. HOMO: highest occupied molecular orbital.

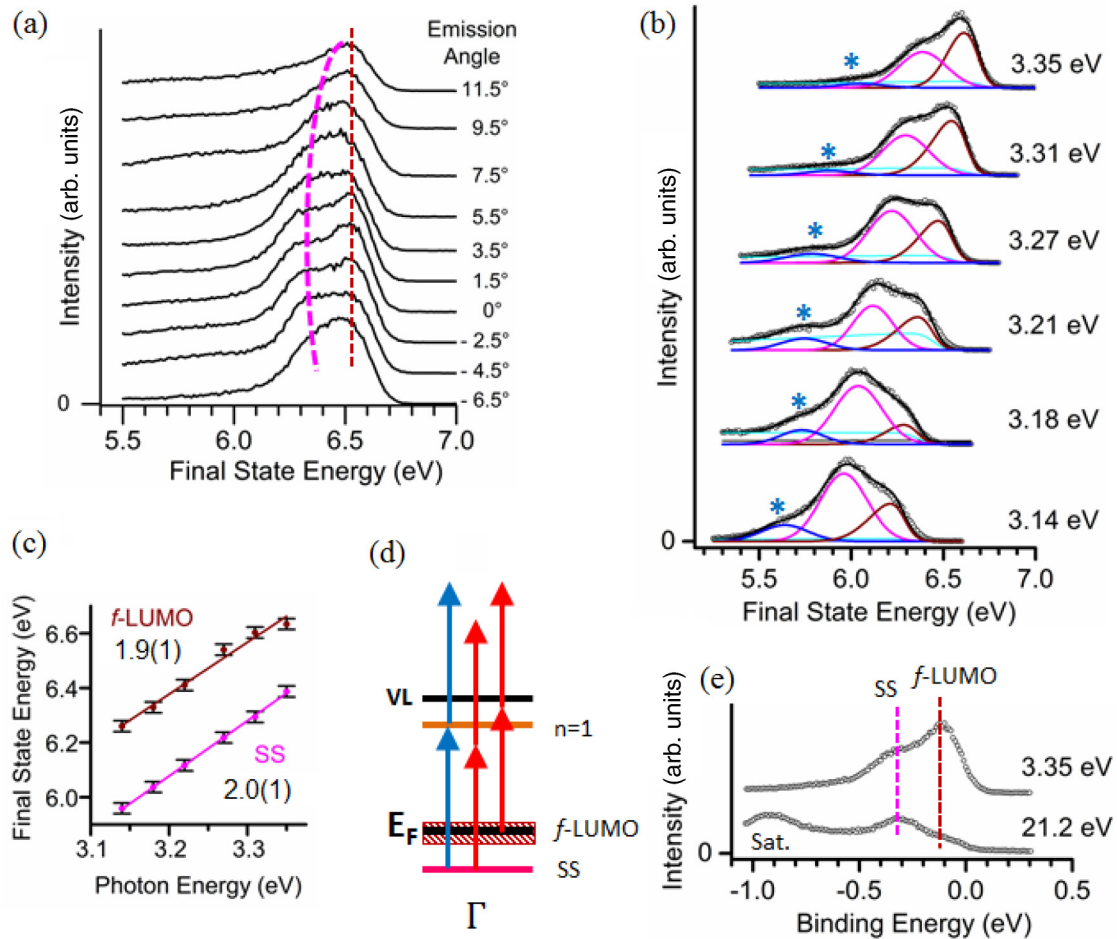


FIG. 6. (Color online) 0.47 MLE CIB-SubPc/Cu(111) TPPE spectra measured (a) at $\hbar\omega = 3.31$ eV and different emission angles and (b) at surface normal and various excitation energies. The photon energy dependence of SS (pink) and f -LUMO (brown) is shown in (c), where the slopes are obtained from linear fits. The symbol * (blue) in (b) represents a state tied to a different (lower) local vacuum level (see text for details). For simplicity, the * state is fit with a symmetric (Gaussian) function. (d) Excitation scheme of SS and f -LUMO, where blue arrows indicate coherent optical resonance between surface state and $n = 1$. (e) Comparison of region near E_F between UP and TPPE spectra.

dependence [slope $\Delta = 2.0(1)$ in Fig. 6(c)] and an identical binding energy in UPS [Fig. 6(e)]. The peak is rapidly quenched and only weakly visible already at 0.85 MLE CIB-SubPc/Cu(111) due to thin film formation and the surface sensitivity of TPPE. For multilayer coverage, the Shockley surface state is no longer detected in the TPPE spectra. Modification and quenching of this state may be caused by surface electron scattering into bulk states at the inhomogeneously distributed adsorbate sites, an induced surface reconstruction upon CIB-SubPc adsorption, or hybridization between the molecular and surface state electronic wave functions [28–30]. Evidence for the latter stems from charge transfer observed at the interface and is discussed in more detail in Sec. IV A.

3. Filled lowest unoccupied molecular orbital

The most striking feature observed appears at submonolayer coverages near the Fermi energy, the filled lowest unoccupied molecular orbital, labeled “ f -LUMO” in Fig. 5. A close-up of this region is shown in Fig. 6(b) for a 0.47 MLE film and as a function of TPPE excitation energy. The TPPE spectra clearly show the presence of two dominant, separate peaks with changing relative intensities, as well as a

small shoulder at lower E_{final} labeled by an asterisk. The lower of the two principal features is the Shockley surface state as discussed in the previous section, while the higher E_{final} feature is the f -LUMO. Figure 6(c) shows that it exhibits a marked two-photon dependence with a slope of $\Delta = 1.9(1)$, indicating that it arises from an occupied level in the presence of CIB-SubPc, with a binding energy of $-0.03(2)$ eV.

The ionization energy of CIB-SubPc is approximately 6 eV [31], i.e., in considerable excess of the global work function [4.40(2)–3.89(2) eV] for all films shown in Fig. 5. This feature can therefore not be easily assigned to the HOMO. A possible interpretation may lie in the heterogeneous growth mode of the room-temperature-grown film, which could in principle support multiple different surface states, on patches of bare Cu(111) and in molecular islands. Indeed, the binding energy of Shockley surface states may shift in response to an adsorbate [32], in some instances even into the unoccupied manifold to energies above E_F [33,34]. This could in principle give rise to an emerging surface state with an apparent binding energy close to E_F . This is, however, not the case, as is clearly seen in Fig. 6(a), where the f -LUMO is distinctly nondispersive, indicating a localized and hence more molecular character.

Close inspection of Fig. 6(b) also shows that the associated peak is asymmetric, bisected by E_F . All these observations taken together strongly suggest charge transfer as its origin, partially filling the CIB-SubPc LUMO and hence labeled f -LUMO. Note that this state is no longer observed at multilayer coverage, in good agreement with the notion that the f -LUMO state originates from charge transfer occurring at the interface between the surface and the molecule. We note as an aside that this state was not detected as clearly in the ultraviolet photoelectron (UP) spectra of the same films [see Fig. 6(e)], although a faint shoulder may be just perceived. We tentatively attribute this to different photoemission cross sections of UPS, making TPPE an invaluable tool in studying the interfacial electronic structure of organic/metal systems.

The observation of the small feature labeled “*” in Fig. 6(b) is attributed to the heterogeneous film growth. The binding energy difference between the f -LUMO and * states ($\Delta E_{\text{final}} = 0.61(2)$ eV) is similar to the global work function difference ($\Delta\Phi = 0.51(2)$ eV) between 0.47 MLE and 0.85 MLE CIB-SubPc/Cu(111). This suggests that this state may thus also correspond to an f -LUMO-like charge-transfer state, located however in a clusterlike chemical environment supporting a lower local vacuum level and thus detected at lower final state energy.

4. Highest occupied molecular orbital

The feature labeled “HOMO” in Fig. 5 represents ionization from the ground state of neutral molecules and is only clearly resolved at multilayer coverage in TPPE. Below 1 MLE, it is suppressed by the secondary electron cutoff at this excitation energy. The measured E_{final} results in an ionization energy of 5.98(4) eV, which is in close agreement with the value of 6.12(2) eV obtained from UPS measurements of CIB-SubPc on highly ordered pyrolytic graphite (HOPG) and 6 eV on Ag(111) [31]. The photon energy dependence of the HOMO feature along the surface normal direction qualitatively agrees with this assignment [slope Δ of 1.62(5) for final state vs photon energy]. Both observations are consistent with an occupied level. The deviation of its slope from a value of 2 will be discussed in Sec. IV.B.

5. Excited states

In Fig. 5, an additional feature labeled “Excit.” is observed very faintly already at 0.47 MLE, emerging more clearly at 0.85 MLE CIB-SubPc/Cu(111). Its slope $\Delta = 1.1(1)$ identifies it as arising from unoccupied levels. The broad width when compared to all other features in the spectra (~ 700 meV) suggests that this feature corresponds to a cluster of closely spaced excited states with energies between ~ 2.0 and 2.5 eV above E_F .

To investigate whether these excited states are excitonic in nature, we compare their relative energetic positions with respect to the f -LUMO and HOMO. The excitation energies used in the TPPE spectra (3.1–3.4 eV) are insufficient to populate these states from the HOMO, let alone lower lying occupied molecular levels. At the same time, their energy is not commensurate with direct excitation from the f -LUMO either.

Hence, these states are likely populated by scattering from Cu(111) electrons and correspond thus to molecular anion states, a hallmark of *strong coupling* between the molecular and surface electronic states [35–38]. Such strong coupling in the first molecular layer may be expected given the formation of an f -LUMO, and it further suggests mixing of molecular and (bulk) electronic states of Cu(111) [39].

6. Image potential states

The feature labeled “IPS” in Fig. 5 shows no photon energy dependence, $\Delta = 0$, and corresponds therefore to a final state resonance. This indicates a discrete state residing above the vacuum level, embedded in the translational continuum of the free photoelectron. In the present case and based on its coverage dependence and final state energy, this feature is, however, attributed to the $n = 2$ IPS of bare Cu(111), with a binding energy pinned to the local vacuum level of a patch of bare surface. As will be discussed in more detail in Sec. IV.B, detection in our TPPE spectrum results from autoionization into the continuum supported above the local vacuum level of islands of CIB-SubPc/Cu(111).

7. Summary of spectroscopy

A careful analysis of coverage- and excitation energy-dependent AR-TPPE spectra, in conjunction with an understanding of the coverage-dependent thin film structure from LT-STM, reveals a molecular HOMO, several excited states, various bare Cu(111) surface-confined states (SS and IPS), and a partially filled f -LUMO. The salient features in these spectra report in detail on the interfacial interactions and point to strong coupling at this interface. This is the main aspect discussed in the following section.

IV. DISCUSSION

A. Charge transfer

Angle-resolved two-photon photoemission spectra of 0.47 MLE CIB-SubPc/Cu(111) measured at $\bar{\Gamma}$ show principally two well-resolved features [Fig. 6(b)] near E_F . The photon energies in these spectra were chosen so as to prevent direct single-photon excitation of the IPSs, reducing spectral congestion and simplifying a careful investigation of the spectral features present. The shape of the envelope unambiguously points to two overlapping peaks, which were further analyzed by carefully fitting the spectra at different excitation energies. A Gaussian peak profile was used to fit both the Shockley surface state and the f -LUMO after a constant linear background subtraction. The f -LUMO was convolved with a Fermi-Dirac distribution representing the Cu sp bands [Fig. 6(b)]. Both states exhibit two-photon dependence with a slope of ~ 2 [Fig. 6(c)] and represent thus occupied states, in agreement with their assignment as the Shockley surface state and the f -LUMO.

All observed attributes of the state labeled f -LUMO suggest strongly that this state is formed by partial electron transfer from Cu(111) to a previously unoccupied state of the molecule: (i) The peak center is very close to E_F , with E_F bisecting the peak; (ii) assignment of this feature as HOMO is incompatible with an ionization energy of approximately 6 eV

reported previously on Ag(111) [31] and measured by us on graphite, given a global work function below 4.5 eV; (iii) the solution HOMO-LUMO gap of ~ 2.2 eV [40] predicts to first approximation a LUMO energy near E_F ; (iv) the localized, nondispersive electronic character is indicative of a molecular level; and (v) the disappearance of this peak at coverages $\rightarrow 1$ MLE is expected for an interface-specific feature arising from charge transfer from the surface to a molecule. Given this interpretation of the f -LUMO, the binding energy of $-0.03(2)$ eV at $k_{\parallel} = 0$ implies transfer of close to a full electron to the molecule and is presumably accompanied by back donation to lower lying molecular orbitals [41].

Such adsorption-induced partial electron transfer from surface to molecules has recently been observed, e.g., for PTCDA, C_{60} , and several other organic molecules on coinage metal surfaces [26,31,35,40,42–46]. In the case of CIB-SubPc on Ag(111), Berner *et al.* [31] inferred a partial charge transfer from surface to molecule from analysis of x-ray photoelectron spectroscopy (XPS) and UPS. This transfer was suggested to be localized on the Cl atom of CIB-SubPc, oriented towards the surface on Ag(111), and it appears to show no effect on the π -system of the molecular ground state.

The combination of STM and photoelectron spectroscopy leads to a different conclusion for CIB-SubPc on Cu(111). The photoemission intensity for the f -LUMO exhibits a distinct angle dependence [Fig. 6(a)], in agreement with the molecular origin of this state. This is likely the result of photoemission selection rules in structured thin films with well-organized adsorption geometries [24,47]. This indicates that the f -LUMO arises from ordered molecular structures on the surface, which from the STM data in Fig. 3 are associated with the high-density, hexagonally packed Cl-up molecules directly at the metal interface. Cl-up, also the preferred orientation at the organic/metal interface for the films and coverages investigated here, is thus very likely the specific molecular adsorption geometry undergoing charge transfer on this surface. This is at variance with the findings on Ag(111), where charge transfer was suggested to be partial and localized to the Cl atom only, believed to be in direct contact with the Ag surface (Cl-down). It is, however, fully consistent with reports of several flat metal phthalocyanines that undergo charge transfer to the π -system as well, and it indicates the more activated nature of the Cu surface. Taken together, the identification of the f -LUMO as originating from partial charge transfer across the interface is indicative of strong coupling of CIB-SubPc to Cu(111), and it may also explain the observed quenching of the Shockley surface state at higher coverages [28].

B. Interface coupling and the image potential manifold

At submonolayer coverages and for a film deposited at room temperature, the molecular organization observed by STM shows abundant ordered structures in the first monolayer consisting of dense hexagonally packed Cl-up molecules, together with more complex heterogeneous growth at coverages close to 1 MLE. The heterogeneous nature of the 3D clusters, some molecular disorder in the wetting layer, and bare areas found on the surface all raise questions about the notion of a global vacuum level, as determined by the secondary electron cutoff

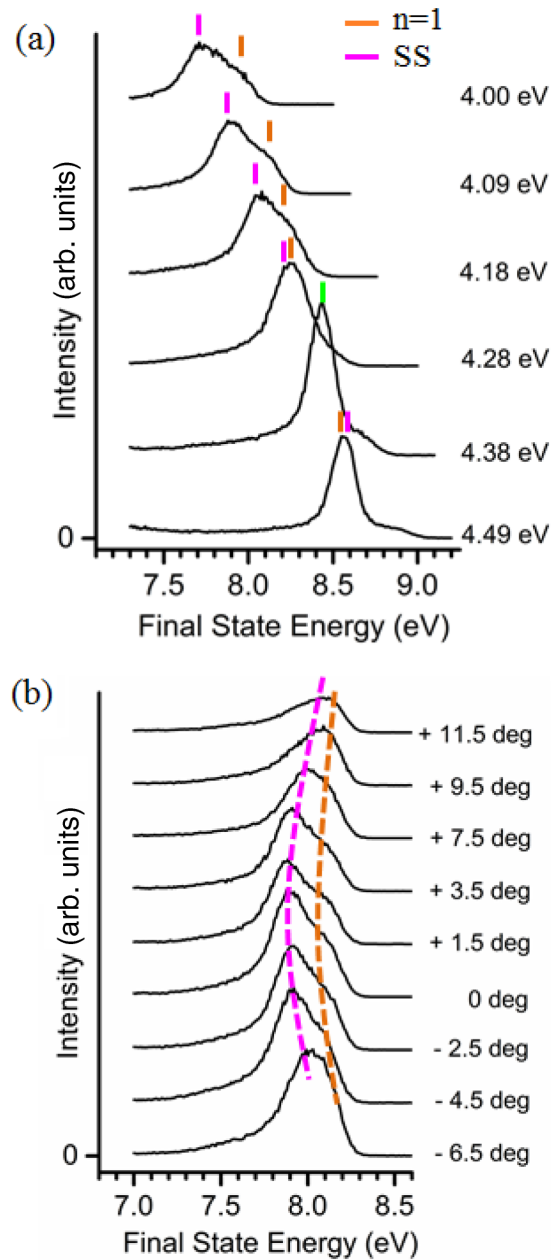


FIG. 7. (Color online) 0.47 MLE TPPE spectra measured (a) at different excitation energies and at $\bar{\Gamma}$, and (b) at $\hbar\omega = 4.09$ eV and different emission angles. An optical resonance between $n = 1$ and Shockley surface state of bare Cu(111) results in a sharp single peak at $\hbar\omega = 4.38$ eV.

in UPS or TPPE, and the meaning of such a global vacuum level in the assignment of the interfacial electronic structure of this system. Indeed, a first indication of the influence and importance of a varying local vacuum level arises already from the $*$ state in Fig. 6(b) and its interpretation as an f -LUMO, providing evidence of multiple different local vacuum levels.

The presence of different local vacuum levels also has a profound effect on the image potential manifold at this interface. When exciting the film at 0.47 MLE coverage with photon energies between 4.0 and 4.5 eV, two features are observed in the AR-TPPE spectra (Fig. 7). Both are

dispersive, with $m_{\text{eff}} \approx 1.0 m_e$ and $m_{\text{eff}} \approx 0.4 m_e$. Together with the dispersion properties, their final state energies identify them as arising from the Shockley surface state and the $n = 1$ IPS, both of bare Cu(111). The $n = 1$ IPS has a binding energy of 0.81(2) eV relative to the bare Cu(111) vacuum level, in good agreement with previous reports [48]. Image potential states are by their very nature pinned to the local vacuum level [38,45,49], and the binding energy depends therefore on the local film morphology. The excitation of $n = 1$ of the bare Cu(111) surface implies the existence of small patches of bare Cu(111), consistent with the STM data of films in this coverage range [Fig. 3(a)]. Note that excitation energies needed to populate the bare Cu(111) $n = 2$ IPS exceed the global work function at 0.47 MLE and lead therefore to spectra dominated by one-photon photoemission, inhibiting a reliable analysis of the associated TPPE spectra. Interestingly, no clear evidence for IPSs on the adsorbate-covered surface patches is observed, which would be expected to appear at lower E_{final} , possibly due to disorder at the interface or a much shortened lifetime at the image potential manifold. Strong coupling to the interface and the formation of anion resonances, as discussed in Sec. III, are fully consistent with a rapid decay of the IPSs formed above CIB-SubPc/Cu(111) islands.

At 0.85 MLE surface coverage of CIB-SubPc on Cu(111), the TPPE spectra are richer in information regarding the interfacial electronic structure, revealing the importance of the local vacuum level. Figure 8 displays angle-integrated TPPE spectra of 0.85 MLE CIB-SubPc/Cu(111), recorded with

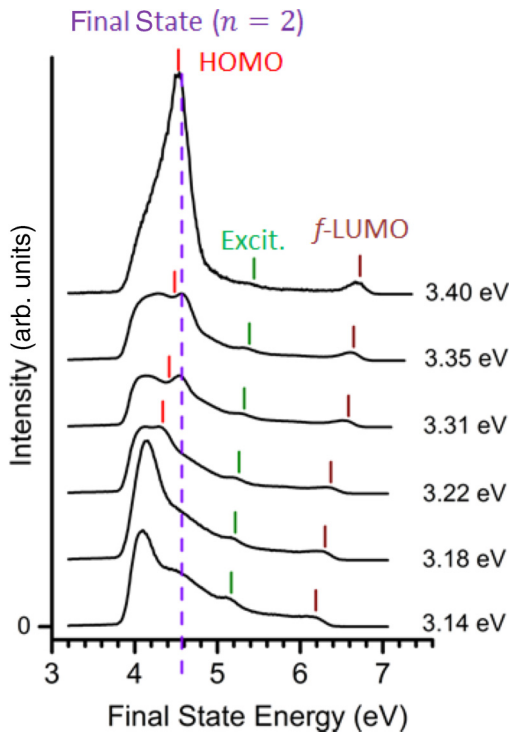


FIG. 8. (Color online) 0.85 MLE CIB-SubPc/Cu(111) TPPE spectra measured at different excitation energies and $0^\circ \pm 12^\circ$ emission angle with respect to the surface normal. The energetic position of the HOMO feature is assigned based on the analysis of TPPE spectra in Fig. 7(a).

excitation energies below the energy needed for one-photon absorption into the image potential manifold of the bare Cu(111) surface. In contrast to TPPE spectra acquired at photon energies between 4.0 and 4.5 eV and for a coverage of 0.47 MLE, excitation of the $n = 1$ IPS of bare Cu(111) in the 0.85 MLE film with photon energies between 3.1 and 3.4 eV results in a final state energy overlapping with the secondary cutoff of the TPPE spectra, and this state can thus not be resolved at this coverage and with the photon energies used.

Aside from the f -LUMO and excited state features, the TPPE spectra at 0.85 MLE show an additional feature close to the secondary electron cutoff. Its lack of a photon-energy dependence of E_{final} ($\Delta = 0$) identifies it as a discrete final state located above the global vacuum level, as was also reported, e.g., for the unoccupied $\pi^* e_{2u}$ state of benzene on Cu(111) [12]. Strikingly, the intensity of this feature appears to increase with larger excitation energies, exhibiting a drastic change when becoming resonant at $\hbar\omega = 3.40$ eV with Cu d -bands, the Tamm state, as well as the HOMO feature (all three with binding energies near ~ -2.2 eV). The final state energy of this state with respect to E_F is 4.56(2) eV, which is well above the global vacuum level [by 0.67(2) eV] in the 0.85 MLE CIB-SubPc film on Cu(111), but 0.31(2) eV below the vacuum level of bare Cu(111). Such a binding energy relative to the Cu(111) vacuum level coincides with the reported binding energy of the $n = 2$ IPS of bare Cu(111) (0.25(7) eV) [50]. Note that we can exclude the possibility that this feature originates from a bulk transition in Cu, since the detected state resides below the known upper band edge of the Cu(111) L-gap [45]. The observation of an IPS as a final state resonance is striking and implies that the $n = 2$ IPS, pinned to the local vacuum level of bare Cu(111), autoionizes by coupling to the continuum arising from neighboring adsorbate-covered areas in the film. This is a direct consequence of the different local vacuum levels present in a thin organic film with complex morphology, and the observation is made possible by the lower local vacuum level of the various CIB-SubPc/Cu(111) patches on the surface. This situation is intimately related to the formation of confined IPSs in the partial second adsorbed layer of benzene on Cu(111) [45], where a local variation of the electron affinity due to a proposed inhomogeneous film structure leads to confinement of the IPS.

The resonance enhancement of $n = 2$ IPS of bare Cu(111) suggests an optical resonance with the bulk d bands or the Tamm surface state of Cu(111). Alternatively, the dramatic increase in the photoemission intensity of the $n = 2$ IPS might be caused by borrowing intensity from direct coherent excitation of the HOMO state into its associated ionization continuum, resonant with the $n = 2$ IPS on bare Cu(111) at a photon energy of 3.40 eV (Fig. 9). Though somewhat speculative at present, such a mechanism is predicated on strong electronic coupling of the molecule with the surface, in agreement with all other spectral observations at this interface. In this case, the electronic interactions \hat{V} between surface and molecule would contain a lateral component, tying the $n = 2$ IPS manifold of bare Cu(111) to the surface/molecule manifold of adsorbate-covered islands. Such interactions are consistent with a HOMO photon dependence of $\Delta = 1.62(5)$,

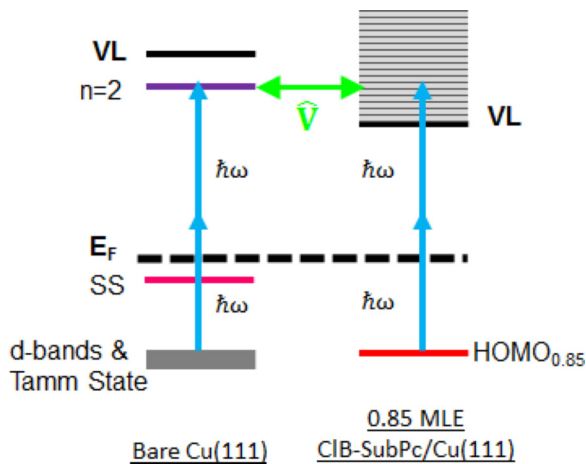


FIG. 9. (Color online) Schematic of intensity borrowing of the final discrete state observed in TPPE spectra of 0.85 MLE CIB-SubPc/Cu(111) resulting from the strong electronic coupling of CIB-SubPc with Cu(111). \hat{V} indicates lateral electronic coupling between $n = 2$ and the continuum.

which is less than the expected $\Delta = 2$ for a regular occupied level.

V. CONCLUSIONS

In summary, we present a comprehensive analysis of the interfacial electronic structure of the initial stages of thin film growth of CIB-SubPc on Cu(111) by TPPE. The combination of LT-STM, UPS, and AR-TPPE allows the interfacial interactions to be disentangled to a considerable degree despite inhomogeneous growth and structural polymorphism exhibited at this interface. The inhomogeneous film growth of CIB-SubPc on Cu(111) gives rise to different local vacuum levels, resulting in the coexistence of different local interfacial

electronic structures that we are able to unravel. In particular, the STM data show orientation-dependent adsorption behavior in CIB-SubPc films, where the Cl-up orientation is favored in the wetting layer. The photoelectron spectroscopy uncovers strong coupling to the surface with charge transfer from the surface to the molecule, resulting in a newly filled f -LUMO located at the Fermi level. The observed charge-transfer state is interface specific and is related to the predominant Cl-up orientation of the molecule on the surface.

Strong interfacial and lateral electronic coupling also results in molecular anion resonances at energies in excess of the f -LUMO and potentially causes intensity borrowing and resonance enhancement of the $n = 2$ IPS of bare Cu(111). The orientation-selective adsorption behavior of CIB-SubPc on Cu(111) and the existence of different local vacuum levels at the interface demonstrate a significant aspect of thin film morphology for understanding surface/molecule interactions. Our results show that it is necessary to closely correlate the molecular detail of film structure with the spectroscopy in order to understand the interfacial electronic structure. This is particularly true in the case of significant structural heterogeneity, but it likely holds more generally, opening the door for detailed investigations of mechanisms for interface dipole formation, energy-level alignment, and charge-transfer dynamics at interfaces even of complex organic thin films.

ACKNOWLEDGMENTS

This work was supported by the National Science Foundation under Grant No. CHE-1213243. LT-STM research was carried out at the Center for Functional Nanomaterials, Brookhaven National Laboratory, which is supported by the U.S. Department of Energy, Office of Basic Energy Sciences, under Contract No. DE-AC02-98CH10886 and under User Proposal No. 31054. We would like to acknowledge Dr. P. Zahl and Dr. P. Sutter for their invaluable help with STM.

- [1] X.-Y. Zhu, *J. Phys. Chem. B* **108**, 8778 (2004).
- [2] F. Flores, J. Ortega, and H. Vázquez, *Phys. Chem. Chem. Phys.* **11**, 8658 (2009).
- [3] S. Braun, W. R. Salaneck, and M. Fahlman, *Adv. Mater.* **21**, 1450 (2009).
- [4] J. V. Barth, *Annu. Rev. Phys. Chem.* **58**, 375 (2007).
- [5] O. L. A. Monti, *J. Phys. Chem. Lett.* **3**, 2342 (2012).
- [6] W. Liu, J. Carrasco, B. Santra, A. Michaelides, M. Scheffler, and A. Tkatchenko, *Phys. Rev. B* **86**, 245405 (2012).
- [7] B. Stadtmüller, I. Kröger, F. Reinert, and C. Kumpf, *Phys. Rev. B* **83**, 085416 (2011).
- [8] M. Toader, M. Knupfer, D. R. T. Zahn, and M. Hietschold, *Surf. Sci.* **605**, 1510 (2011).
- [9] S. Duhm, A. Gerlach, I. Salzmänn, B. Bröker, R. L. Johnson, F. Schreiber, and N. Koch, *Org. Elec.* **9**, 111 (2008).
- [10] M. Wießner, D. Hauschild, A. Schöll, F. Reinert, V. Feyer, K. Winkler, and B. Krömker, *Phys. Rev. B* **86**, 045417 (2012).
- [11] M. L. Blumenfeld, M. P. Steele, and O. L. A. Monti, *J. Phys. Chem. Lett.* **1**, 145 (2010).
- [12] S. Duhm, G. Heimel, I. Salzmänn, H. Glowatzki, R. L. Johnson, A. Völlmer, J. P. Rabe, and N. Koch, *Nat. Mater.* **7**, 326 (2008).
- [13] I. Salzmänn, S. Duhm, G. Heimel, M. Oehzelt, R. Kniprath, R. L. Johnson, J. P. Rabe, and N. Koch, *J. Am. Chem. Soc.* **130**, 12870 (2008).
- [14] A. Tamai, A. P. Seitsonen, F. Baumberger, M. Hengsberger, Z.-X. Shen, T. Greber, and J. Osterwalder, *Phys. Rev. B* **77**, 075134 (2008).
- [15] A. Schöll, L. Kilian, Y. Zou, J. Ziroff, S. Hame, F. Reinert, E. Umbach, and R. H. Fink, *Science* **329**, 303 (2010).
- [16] N. Balke, D. Bonnell, D. S. Ginger, and M. Kemerink, *MRS Bull.* **37**, 633 (2012).
- [17] P. Zahl, M. Bierkandt, S. Schröder, and A. Klust, *Rev. Sci. Instr.* **74**, 1222 (2003).
- [18] T. Fauster, M. Weinelt, and U. Höfer, *Prog. Surf. Sci.* **82**, 224 (2007).
- [19] N. Ilyas, L. L. Kelly, and O. L. A. Monti, *Mol. Phys.* **111**, 2175 (2013).
- [20] C. Kentsch, M. Kutschera, M. Weinelt, T. Fauster, and M. Rohlfing, *Phys. Rev. B* **65**, 035323 (2001).
- [21] A. Jablonski and K. Wandelt, *Surf. Interface Anal.* **17**, 611 (1991).
- [22] H. Ishii, K. Sugiyama, E. Ito, and K. Seki, *Adv. Mater.* **11**, 605 (1999).

- [23] O. L. A. Monti and M. P. Steele, *Phys. Chem. Chem. Phys.* **12**, 12390 (2010).
- [24] S. Kera, H. Yamane, H. Fukagawa, T. Hanatani, K. K. Okudaira, K. Seki, and N. Ueno, *J. Electron Spectrosc. Relat. Phenom.* **156**, 135 (2007).
- [25] G. M. Rangger, O. T. Hofmann, L. Romaner, G. Heimel, B. Broeker, R.-P. Blum, R. L. Johnson, N. Koch, and E. Zojer, *Phys. Rev. B* **79**, 165306 (2009).
- [26] Y. Zou, L. Kilian, A. Schöll, T. Schmidt, R. Fink, and E. Umbach, *Surf. Sci.* **600**, 1240 (2006).
- [27] A. Terentjevs, M. P. Steele, M. L. Blumenfeld, N. Ilyas, L. L. Kelly, E. Fabiano, O. L. A. Monti, and F. Della Sala, *J. Phys. Chem. C* **115**, 21128 (2011).
- [28] F. Baumberger, T. Greber, B. Delley, and J. Osterwalder, *Phys. Rev. Lett.* **88**, 237601 (2002).
- [29] A. Nuber, M. Higashiguchi, F. Forster, P. Blaha, K. Shimada, and F. Reinert, *Phys. Rev. B* **78**, 195412 (2008).
- [30] P. Borghetti, J. Lobo-Checa, E. Goiri, A. Mugarza, F. Schiller, J. E. Ortega, and E. E. Krasovskii, *J. Phys.: Condens. Matter* **24**, 395006 (2012).
- [31] S. Berner, M. de Wild, L. Ramoino, S. Ivan, A. Baratoff, H.-J. Güntherodt, H. Suzuki, D. Schlettwein, and T. A. Jung, *Phys. Rev. B* **68**, 115410 (2003).
- [32] J. Ziroff, P. Gold, A. Bendounan, F. Forster, and F. Reinert, *Surf. Sci.* **603**, 354 (2009).
- [33] C. H. Schwalb, S. Sachs, M. Marks, A. Scholl, F. Reinert, E. Umbach, and U. Hofer, *Phys. Rev. Lett.* **101**, 146801 (2008).
- [34] B. W. Caplins, D. E. Suich, A. J. Shearer, and C. B. Harris, *J. Phys. Chem. Lett.* **5**, 1679 (2014).
- [35] P. Amsalem, J. Niederhausen, J. Frisch, A. Wilke, B. Bröker, A. Vollmer, R. Rieger, K. Müllen, J. P. Rabe, and N. Koch, *J. Phys. Chem. C* **115**, 17503 (2011).
- [36] G. Dutton and X. Y. Zhu, *J. Phys. Chem. B* **105**, 10912 (2001).
- [37] C. Gahl, K. Ishioka, Q. Zhong, A. Hotzel, and M. Wolf, *Faraday Discuss.* **117**, 191 (2000).
- [38] M. P. Steele, M. L. Blumenfeld, and O. L. A. Monti, *J. Chem. Phys.* **133**, 124701 (2010).
- [39] E. Varene, I. Martin, and P. Tegeder, *J. Phys. Chem. Lett.* **2**, 252 (2011).
- [40] G. E. Morse and T. P. Bender, *ACS Appl. Mater. Interfaces* **4**, 5055 (2012).
- [41] O. T. Hofmann, V. Atalla, N. Moll, P. Rinke, and M. Scheffler, *New J. Phys.* **15**, 123028 (2013).
- [42] C.-T. Tzeng, W.-S. Lo, J.-Y. Yuh, R.-Y. Chu, and K.-D. Tsuei, *Phys. Rev. B* **61**, 2263 (2000).
- [43] G. K. Wertheim and D. N. E. Buchanan, *Phys. Rev. B* **50**, 11070 (1994).
- [44] J. Niederhausen, P. Amsalem, A. Wilke, R. Schlesinger, S. Winkler, A. Vollmer, J. P. Rabe, and N. Koch, *Phys. Rev. B* **86**, 081411 (2012).
- [45] D. Velic, A. Hotzel, M. Wolf, and G. Ertl, *J. Chem. Phys.* **109**, 9155 (1998).
- [46] F. S. Tautz, M. Eremitchenko, J. A. Schaefer, M. Sokolowski, V. Shklover, and E. Umbach, *Phys. Rev. B* **65**, 125405 (2002).
- [47] S. Hasegawa, S. Tanaka, Y. Yamashita, H. Inokuchi, H. Fujimoto, K. Kamiya, K. Seki, and N. Ueno, *Phys. Rev. B* **48**, 2596 (1993).
- [48] S. Schuppler, N. Fischer, T. Fauster, and W. Steinmann, *Phys. Rev. B* **46**, 13539 (1992).
- [49] A. Yang, S. T. Shipman, S. Garrett-Roe, J. Johns, M. Strader, P. Szymanski, E. Muller, and C. Harris, *J. Phys. Chem. C* **112**, 2506 (2008).
- [50] M. Wolf, E. Knoesel, and T. Hertel, *Phys. Rev. B* **54**, R5295 (1996).